

DISCLAIMER

This report was prepared as an account of work sponsored by an agency of the United States Government. Neither the United States Government nor any agency thereof, nor any of their employees, makes any warranty, express or implied, or assumes any legal liability or responsibility for the accuracy, completeness, or usefulness of any information, apparatus, product, or process disclosed, or represents that its use would not infringe privately owned rights. Reference herein to any specific commercial product, process, or service by trade name, trademark, manufacturer, or otherwise, does not necessarily constitute or imply its endorsement, recommendation, or favoring by the United States Government or any agency thereof. The views and opinions of authors expressed herein do not necessarily state or reflect those of the United States Government or any agency thereof.

Printed in the United States of America. Available from:
National Technical Information Service
U.S. Department of Commerce
5285 Port Royal Road
Springfield, VA 22161

NTIS price codes
Paper copy: **A03**
Microfiche copy: **A01**

NIPER-378
Distribution Category UC-122

DETERMINING PETROPHYSICAL PROPERTIES OF RESERVOIR
ROCKS BY IMAGE ANALYSIS

Topical Report

By
Liviu Tomutsa
Alan Brinkmeyer
Clarence Raible

March 1989

Work Performed Under Cooperative Agreement No. FC22-83FE60149

Prepared for
U.S. Department of Energy
Assistant Secretary for Fossil Energy

Alex Crawley, Project Manager
Bartlesville Project Office
P.O. Box 1398
Bartlesville, OK 74005

Prepared by
IIT Research Institute
National Institute for Petroleum and Energy Research
P.O. Box 2128
Bartlesville, OK 74005

TABLE OF CONTENTS

	<u>Page</u>
Abstract.....	1
Introduction.....	1
Experimental.....	2
Equipment.....	2
Methodology Investigations for Pore structure and Microscopic Images.....	4
Selection of Rock Samples for PIA Investigations.....	4
Thin Section Preparation.....	5
Methods for Improving Microscopic Images.....	5
SEM Photographs.....	6
Fluorescent Images.....	6
Size Calibration of Image Analysis System.....	8
Image Capture and Feature Detection.....	9
Petrophysical Properties Measured by PIA.....	9
Procedures for Petrophysical Measurements.....	10
Correlation of Porosity Data.....	10
Rock Grain Measurements.....	11
Methods for Permeability Estimation.....	12
Discussion and Conclusions.....	14
References.....	15

TABLES

1. Measurements of microsphere diameters by image analysis.....	16
2. Porosity measured by volumetric analysis of core plugs and porosity from thin section PIA.....	17
3. Measurements of rock grains for maximum and minimum mean diameters and mean grain area.....	18
4. Comparison of grain area with elliptical area based on maximum and minimum grain diameters.....	19
5. Comparison of porosity and permeability obtained by PIA with those obtained by core plug analysis using the Kozeny constant of 5.....	20

ILLUSTRATIONS

1. SEM backscattered electron image of epoxy pore cast of a sample from Bell Creek field, Powder River County, Montana.....	21
2. Pixel intensity histogram showing contrast of images captured using glass and fluorite objectives.....	22
3. An example of image analysis porosity variation due to thin section heterogeneities.....	23

4a. Correlation of image analysis porosity versus volumetric core-plug porosity for Muddy formation.....	24
4b. Correlation of image analysis porosity versus volumetric core-plug porosity for Shannon formation.....	24
5a. Histogram of pixel gray-level for fluorescent image of a "clean" sandstone.....	25
5b. Histogram of pixel gray-level for a fluorescent image of a low-porosity sandstone containing large quantities of clays and silty materials.....	25
6. Comparison of grain areas for two thin sections from subsurface (W11-4378.7) and outcrop (22-100-12.5).....	26
7. Comparison of elliptical area based on maximum and minimum grain diameters with measured grain areas.....	27

DETERMINING PETROPHYSICAL PROPERTIES OF RESERVOIR ROCKS BY IMAGE ANALYSIS

By Liviu Tomutsa, Alan Brinkmeyer, and Clarence Raible

ABSTRACT

The objective of this work is to study pore structures and develop methods for computerized petrographic image analysis to quantify the relationships between pore parameters and petrophysical properties of reservoir rocks. Reservoir properties of oil- and gas-bearing formations are to a large extent dependent on the pore geometry of rocks. Petrographic image analysis (PIA) offers a relatively new technique for measurements of shapes, surface areas, and size distributions of rock pores and size/shape of rock grains. We have developed a methodology for measuring each of these petrophysical features using commercially available equipment. This information can be used to describe porosity and lithologic heterogeneities within a reservoir.

Permeability is a function of the three-dimensional pore network in a rock and cannot be measured directly from two-dimensional PIA data. However, rock parameters, such as porosity and specific surface values, can be measured by PIA. These values are related to permeability. We have used the Carman-Kozeny model for flow-through porous media to estimate permeability using PIA data for porosity and specific surface.

This report describes the equipment and software necessary for image analyses, the application of image data to measurements of rock properties, and the initial correlation of image analysis data to petrophysical properties. This report represents the completion of milestone 8 of the FY88 work plan for Project BE12A and covers the work performed during FY88.

INTRODUCTION

Efficient oil and gas production requires a comprehensive knowledge of the reservoir rock structure. Descriptions of the reservoir rock at various scales are necessary to construct a unified picture for characterizing the reservoir to allow for selection of appropriate strategies in the recovery of oil and gas resources.

Thin section optical microscopy and scanning electron microscopy are

traditional tools used by the petrographer to describe rock properties, including grain size, sorting, cementing materials, pore size, and mineralogy. These parameters are typically qualitative descriptions of rock features. Quantitative measurements involving point counting of grain size are repetitious and time-consuming and require the dedicated attention of a skilled petrographer. The latest advances in computer and video technology allow the use of desk-top computers to capture and analyze petrographic images. Although the use of petrographic image analysis (PIA) does not eliminate the need for a professional petrographer to select features to be measured, PIA does allow increased measurement speed and enhances measurement accuracy. Thus more data can be developed for a statistically correct description of the rock structure.

EXPERIMENTAL

Equipment

The equipment for PIA requires a microscope to obtain a magnified image, a video camera to detect the image, a video image processor to digitize and store the image, and software to perform feature measurements.

The system used for these investigations consists of the following components:

- (1) a Nikon™ petrographic microscope equipped with a transmitted light source and an incident UV light attachment;
- (2) a high-resolution Dage MTI™ black and white video camera capable of detecting low-intensity light images;
- (3) an image analysis hardware and software system procured from American Innovision, Inc.™; and
- (4) a PC Limited AT™ computer used as the host computer for system control, data storage, and image processing.

The petrographic microscope was equipped with an incident light UV lamp attachment as an excitation source for fluorescent samples. Fluorescent images offer some advantages in petrographic image analysis, including better contrast between the pore-rock matrix and reduction of errors associated with transmitted light images. In addition to the glass objectives, a fluorite objective was procured to improve the light intensity of fluorescent images.

The Dage MTI video camera was acquired specifically to capture ultra-low-light intensity images (10^{-2} lux). The video camera has a resolution capability of greater than 1,000 lines and the capability for automatic and manual adjustment for light sensitivity. The manual sensitivity adjustment allows the operator to optimize the camera sensitivity for variations in the fluorescent image intensity between different thin sections. The camera has proved to be a valuable tool for capturing fluorescent images with high video contrast.

The camera does not have color capability. Color cameras with high-resolution and ultra-low-light sensitivity are not available at a reasonable cost. Presently, we have a low-resolution (less than 240-line) Magnavox™ color camera. This camera is not adequate to make accurate comparisons of transmitted light or color images with the gray level images obtained with the Dage MTI camera. Tests were made to compare the color images with those of the Dage MTI camera. Surface area values obtained for the color images were erroneously high as a result of the low resolution of the color camera.

The image analysis hardware and software were procured from American Innovision, Inc. The hardware has color capability with three eight bit color channels/pixel (640x480x24 bit). The 640 line by 480 pixel hardware provides the resolution capability which is adequate for the purposes of this project.

One major advantage of this system is the flexibility for programming the operational steps for automatic execution using a "J" language series of commands. The results of the measurements can be stored in ASCII files from which they can be accessed for further mathematical manipulation and graphic display using plotting and statistical analysis software such as Lotus 123™ or Stratgraphics™.

Some of the operational features of the software package include:

- (1) manual adjustment of the pixel intensity threshold to create a binary image;
- (2) erosion/dilation operation of binary images; and
- (3) feature measurements, including x and y feret diameters, centroids, areas, and the number of features.

At our request, American Innovision Inc. has added the following feature

measurements to the software package:

- (1) radius and direction from the centroid to the perimeter (used to measure the maximum and minimum diameters of a feature) and
- (2) feature perimeter (used to measure the 2-dimensional "surface area" or roughness of pores or grains).

The hardware and software arrived with some operational "bugs". American Innovision was prompt in fixing most of the problems although delays were experienced in achieving operational status of the system. One hardware problem remains to be corrected. This problem is associated with the software code of a ROM chip which counts the number of pixels for area measurements. At present, we are aware of this hardware "bug", and corrections can be made for area measurements. An updated version to eliminate the hardware "bug" is scheduled to be delivered in the fall of 1988.

Methodology Investigations for Pore Structure and Microscopic Images

There are basically three steps in obtaining petrographic parameters by PIA: sample preparation for microscopic examination, microscopic image acquisition, and detection and analysis of image features. All of these steps are interrelated to successfully obtain accurate petrographic information. The quality of the microscopic image has a direct effect on the image analysis system to accurately discriminate between rock features such as the pore/matrix interface. Much of this work involved preparation of rock samples and methods for obtaining microscopic images with sharp contrast between the pore/matrix interface.

The following is a description of some of the investigations performed to improve and obtain quality images with sharp light intensity contrast.

Selection of Rock Samples for PIA Investigations

Rock samples from the Bell Creek reservoir were chosen for initial investigations of this project. Cores from Bell Creek were available with a wide variety of petrographic features including cores with high porosity and permeability values. In addition, some petrographic information for these cores was available from the NIPER Reservoir Characterization Project¹. In the future, information derived from PIA may be used in further characterizing

the Bell Creek reservoir.

Thin Section Preparation

Several thin sections were available for rock samples of the Bell Creek reservoir. Examinations showed that some of these thin sections contain grinding materials and gas bubbles trapped in the impregnated epoxy resin. Grinding materials embedded in thin sections reduce the contrast between rock grains and pores. Gas bubbles trapped in the epoxy resin can be misidentified as rock grains by image analysis.

Several sets of thin sections representing various facies from the Bell Creek and Muddy formations were prepared by another vendor to determine if higher quality thin sections could be obtained from a different source. Also, single- and double-polished thin sections were made to determine if the additional cost is warranted. With transmitted light, the images obtained from "regular" thin sections are inferior compared to the single- and double-polished thin sections which have a much brighter and cleaner appearance. With UV fluorescence, the normal thin sections yielded a lower quality image, but no significant difference was observed between single- and double-polished thin sections. Trapped contaminants in the regular thin sections made PIA measurements untrustworthy. We concluded that single-polished thin sections would be the best choice for PIA, considering cost and thin section quality.

Methods for Improving Microscopic Images

Microscopic images obtained using transmitted light have the advantage of producing color images which may allow for detection and identification of minerals, blue epoxy resin impregnated pores, and other sedimentary features such as silt sized materials. However, the problems associated with image acquisition of thin sections using transmitted light are a primary limitation for correctly detecting features by PIA. Typically, rock samples are impregnated with blue epoxy resin before thin section preparation. The blue colored epoxy resin is used to enhance the appearance of the pore space.

For thin sections, the epoxy resin impregnation can be extremely thin at the rock/pore interface which results in a shelf effect. Consequently, the light intensity contrast for transmitted light is often insufficient to accurately define grain boundaries. Also, transmitted light generates an image that is a cumulative projection of the grains and pores; therefore, the

resultant image is not a true two-dimensional cross section of the rock (Holmes effect). Therefore, investigations of alternative sample preparation and image acquisition methods were made to improve contrast for accurate feature detection.

Several methods were considered for improving image contrast. These methods included images obtained using incident fluorescent light of epoxy-impregnated rocks and scanning electron microscope (SEM) photographs of back-scattered electron images of rock sections and rock pore casts. Each technique may offer advantages for obtaining representative and accurate image features.

SEM Photographs

Figure 1 shows an example of a backscattered electron image of a pore cast taken from the Bell Creek reservoir (well 16, depth 4,328.5 ft). The SEM backscattered electron image shows excellent detail of not only the larger pores (A) and pore connectivity (B), but also smaller secondary porosity (C) resulting from silt and clay inclusions. These photographs also have an inherent three-dimensional quality. Epoxy-resin-impregnated samples which have been polished flat but not etched would be much quicker to prepare and would provide sharper grain boundaries. However, preliminary backscattered electron images from samples prepared in this manner are disappointing with regard to contrast between pore and grain bodies. To use the backscattered electron images and obtain reliable results, we would have to upgrade our SEM hardware. Although there are advantages to the pore cast and polished slab method, the additional time required to prepare pore casts does not justify their use for initial image studies. Pore casts may be used in future work when image analysis techniques are developed more fully.

Fluorescent Images

Fluorescent light images may be one of the more appropriate methods for obtaining microscopic images. Therefore, most of our effort was concentrated on investigating fluorescent techniques. One difficulty with fluorescent light images is the relatively low light intensity. This problem was partly solved by the purchase of an ultra-low light, black and white video camera. Our experience has shown that the epoxy resin used to impregnate thin sections

can vary in inherent fluorescence. For some epoxy resins, the inherent fluorescence yields sufficient contrast, whereas other epoxy resins provide insufficient contrast to define the pore or rock boundaries.

Three avenues were investigated to improve fluorescent image contrast: (1) selection of an optimum excitation filter for the microscope, (2) selection of the microscope objective, and (3) addition of fluorescent stain to the thin sections.

The first approach for sample fluorescence enhancements was to match the incident light wavelength necessary to achieve fluorescent excitation in the sample. Four excitation filters were tested for UV, blue-violet, blue, and green wavelengths. These tests indicated that the green filter produced the highest fluorescence intensity in the epoxy-resin-impregnated thin sections.

The second approach was to select an appropriate objective for the microscope. The fluorescent intensity and contrast of the fluorescent image were improved by the acquisition of a fluorite objective. The advantage of the fluorite objective is a larger aperture and a higher transmission ratio of the incident and reflected (fluorescent) light. The fluorite objective produced higher fluorescent images and better image contrast than the glass objectives used previously.

An example of the difference between the fluorite and glass objectives is shown in figure 2. The figure shows a histogram of pixel intensity for captured images. The pixel intensity value is related to the gray level in the image, zero representing black and 255 representing pure white. In these images the grains are dark (low pixel intensity), and the pores are bright (high pixel value). The fluorite image has significantly higher fluorescent intensity and better pore/grain contrast. For thin section W4-4416.7, there was no clear transition zone between rock pores and rock grains when the glass objective was used.

The third approach was to increase epoxy resin fluorescence using dyes and stains. Some fluorescent materials did not mix uniformly with the resin and resulted in patchy fluorescence. The fluorescent dyes also tended to be water soluble which added to the cost of preparing thin sections. We have found that rhodamine B mixes well with the epoxy resins. This mixture can be used to impregnate thin sections that result in highly fluorescent images.

Several fluorescent stains were tested to enhance fluorescence of the impregnated epoxy resins. A red stain (PSTF Brite Fluorite Red Concentrate) significantly increased epoxy resin fluorescence which resulted in good image contrast between the epoxy-impregnated pores and rock matrix. However, the stain also coated some of the clays and silty infilling materials. This resulted in fluorescence of areas which were not pores and produced erroneously high porosity values. The staining technique can only be used for relatively "clean" rocks which have low clay content.

With the proper combination of the excitation filter and microscope objective, a strong enhancement of the contrast between the pores and rock matrix was obtained in all of the thin sections. However, the use of a fluorescent stain does not appear to be a viable method to increase image contrast for rocks containing clays.

Size Calibration of Image Analysis System

A necessary step for measuring features by image analysis is the calibration of the pixel size in micrometers (μm) for various microscope objectives. Glass slides with calibration grids were acquired from Edmund Scientific Inc. as calibration standards. Grids were used with scales of 100, 10, and 2 μm /division, depending on the magnification of the microscope objectives.

A set of polystyrene beads (microspheres) from Duke Scientific was used to verify the capability of the image analysis system to accurately measure feature size. Samples of microspheres have a relatively narrow size distribution, and these spherical beads are often used by industry as size standards. Four different bead sizes (mean diameter of 32.2, 9.8, 6.8 and 3.8 μm) were measured by image analysis. The measured dimensions closely agree with the dimensions specified by the manufacturer. These results are listed in table 1. It is evident that the image analysis system is capable of accurately measuring small feature dimensions. The practical limit of feature size measurement is approximately 1 μm because of optical aberrations of the microscope and pixel resolution of the image capture system.

Image Capture and Feature Detection

For accurate feature measurements, sufficient contrast must be present between the features and the surrounding background. A threshold value for pixel light intensity must then be selected to differentiate between the features and background.

The video camera gain affects the size of detected features. Initial measurements in this study were made by using an automatic gain for camera sensitivity. This resulted in overemphasizing weak intensity pixels. For fluorescent pores, the automatic mode resulted in capture of pore images which were larger than the actual pore size. Therefore, it was necessary to manually adjust the camera gain to obtain images of proper size.

There is an interdependence between the camera sensitivity level and the threshold value selection. Adjustment of the camera to a high gain or setting the threshold to a low value will result in erroneously high porosity measurements.

One procedure for adjusting the camera gain and setting the threshold value is by visual observation of the image through the petrographic microscope. Although this method gives reasonably accurate measurements, it requires the operator to repeatedly observe and compare the image from the microscope eye piece and the image from the CRT monitor, which is a tedious procedure.

In this work, two CRT monitors were used to assist the operator in making threshold adjustments. One CRT monitor was used to display the captured image stored in the image analysis system. The other CRT monitor was used to view a "live" image from the microscope and video camera. The two images displayed simultaneously allowed the operator to make threshold adjustments for the stored image while viewing the image from the microscope. This greatly assisted the operator by improving the speed and the accuracy in setting the image threshold.

Petrophysical Properties Measured by PIA

A number of petrophysical parameters of thin sections were measured by PIA. These parameters were used to determine porosity, pore surface area, and

grain shape and size distribution. In addition, preliminary estimates of permeability were made using Carman-Kozeny approximations.

Procedures for Petrophysical Measurements

To some extent, all cores contain heterogeneities and, depending on the pore size and magnification, microscopic image analysis represents only a small area of the core sample. Many petrophysical properties such as porosity represent an average of these heterogeneities. Therefore, to obtain a representative measurement, a number of images must be captured and analyzed for each thin section. For homogeneous samples, fewer images are required to obtain a representative statistical average. Also, when high image magnification is used, more images are required to obtain a statistical average.

Figure 3 shows pore area fractions measured for 35 captured images from a thin section with the 10X objective. This figure shows the variation in porosity of randomly captured images due to the rock heterogeneities. To measure porosity by image analysis, it is necessary to average a number of pore images. For porosity measurements in these investigations, 25 to 40 pore images were averaged for each thin section depending on image magnification.

Adjustment of the threshold for each captured image is a time-consuming process. A less time-consuming process involves setting a single threshold for each thin section. Essentially no difference was obtained for the average pore area fraction by the two methods. By using the single threshold technique, the operator can move the thin section to a different location refocus the microscope and initiate the computer to capture, measure the image, and store the data in a data file. A computer program has been written whereby these last three steps are performed automatically. After the desired number of images has been analyzed, the data are averaged to obtain an average data set. The automated procedure using a single threshold greatly increases data acquisition speed.

Correlation of Porosity Data

Thin sections from Muddy and Shannon formation outcrops and the cores from the Hartzog Draw and Naval Reserve fields (Shannon formation) were analyzed by image analysis and compared to volumetric core plug porosity (table 2, figure

4a). For the Hartzog Draw data, the disagreement between the volumetric porosity and the PIA porosity might be due to the fact that the thin sections for PIA porosity measurements had to be prepared from rock samples taken from different locations than the original core plugs, due to lack of availability of these plugs. Due to the heterogeneity of this formation such variations in porosity and permeability are possible even over small distances. For the relatively clean sands from the Muddy formation a good correlation was obtained (figure 4a). A lower correlation was obtained for samples from the Shannon formation (figure 4b) which typically have higher concentrations of interstitial materials (clays and silt-sized particles).

There are a number of reasons for a lower correlation of "dirty" sands. Greater variability between the conventional and image analysis porosity was partially due to sample heterogeneity. The thin section may be less representative of the average porosity obtained by volumetric core-plug analysis. Another factor affecting the correlation is the quality of the captured image. Better contrast between the pores and rock matrix for clean sands than for sandstones containing significant amounts of clays allows for straightforward selection of the gray-level threshold. An example of a clean sand image is shown in figure 5a by a gray-level histogram. This is contrasted in figure 5b by a low porosity "dirty" sand image where the sample contains large quantities of interstitial clays and silt-sized materials. The limitations for image analysis to accurately measuring small pores may also affect accuracy in porosity measurements because features smaller than a few microns are poorly resolved in the digitized image from the light microscope. The actual gray-level threshold is masked by small pores of low light intensity.

Further efforts to improve the image contrast between the clays and silt sized materials and the epoxy-impregnated pores have not been successful. The application of a fluorescent stain to the thin section resulted in an increase in pixel intensity of clay materials. The stain application coated some of the silt and clay materials. This further reduced the contrast between small pores and the interstitial silt sized materials.

Rock Grain Measurements

PIA can be used to measure grain sizes and grain shapes. With proper

software and sufficient feature contrast, PIA can readily measure the grains for maximum/minimum diameters, perimeter, and areas by using thin sections.

The results for grain size measurements for medium-grain-sized rocks are listed in table 3. The data show the mean values for grain area, maximum and minimum diameters, and the grain perimeter for an average of 600 grains per thin section. This type of information is useful for making statistical comparisons of different rocks such as grain size distributions.

An example of grain size distribution is shown in figure 6 where the number of grains is plotted versus grain area for thin sections of similar facies from subsurface and outcrop Muddy formation samples. The figure shows that the particle area is not a normal distribution.

There are many methods to characterize grain shape, but it is extremely difficult to define shapes in a precise manner. Many measures of shape have been proposed based on axial lengths, perimeters, and areas.² However, no measure has proved to be entirely satisfactory in describing shape properties. PIA is capable of measuring any number of shape factors to characterize a geological sequence.

One method of characterizing grain shapes involves comparing the grain area with the area of an ellipse based on the maximum and minimum grain diameters. Figure 7 shows a comparison of the grain areas and the elliptical areas measured by PIA. The figure shows there is a close similarity of the rock grains to an elliptical shape for this rock. Table 4 lists similar comparisons for a number of rock thin sections which shows the rock grains are closely related to an elliptical shape.

These are examples of data obtained by PIA which can be used to characterize rocks of a geological sequence or facies.

Methods for Permeability Estimation

Fluid permeability is an important property of porous rocks which is related to the three-dimensional structure of the pore system. PIA is limited to two-dimensional measurements of rock sections, and PIA cannot directly measure the pore features to determine permeability. Various researchers have attempted to predict permeability of porous media by measuring the pore dimensions. These predictions are based on the assumption that the porous

media are a bundle of capillary tubes with equal cross sectional areas or hydraulic diameters. One form of these predictions is the Carman-Kozeny³ equation for permeability.

$$k_{ck} = \frac{\phi^3}{k_0 (Le/L)^2 (1-\phi)^2 S_0^2} \quad (1)$$

where: ϕ = porosity
 $(Le/L)^2$ = tortuosity
 k_0 = shape factor of the capillaries
 S_0 = specific surface area of the capillaries

The combined factor for $K_0 (Le/L)^2$ is often referred to as the "Kozeny constant." Carman⁴ determined experimentally that the combined factor for $K_0 (Le/L)^2$ is approximately 5 for fluid flow through packs of spherical glass beads. Using an approximate value of 5, equation 1 can be further simplified.

$$k_{ck} = \frac{\phi^3}{5(1-\phi)^2 S_0^2} \quad (2)$$

The variables of equation 2 are expressed in units which can be measured by PIA. The equation can be used as a simple approximation for estimating permeability from porosity and surface area data obtained by PIA.

Specific surface areas (S_0) were computed from PIA data by the relationship:

$$S_0 = \frac{4 \text{ pore perimeter}}{\pi \text{ pore area}} \quad (3)$$

The specific surface increases with greater magnification because more details of the pore perimeters are resolved. Thus the magnification selected must be sufficient to resolve most of the pores which conduct flow, and an appropriate magnification must be used to measure a specific surface value which is representative for the Carman-Kozeny approximation.

Table 5 compares measured air permeabilities with those calculated from the Carman-Kozeny equation using the 5X and the 10X objectives. The PIA

permeabilities calculated for the 5X objective are closer to the plug measured values because the surface areas measured for the 5X objective are more suitable for the Carman-Kozeny capillary tube model.

The approximations for tortuosity and shape factor used to obtain k_{ck} appear to be unavoidable. The approximations used in the Carman-Kozeny equation may not be valid if the actual tortuosity of the rock is difficult to estimate, and the results for k_{ck} may be erroneous. The Kozeny constant may be modified by further work to obtain empirically derived values. Such values for the Kozeny constant may yield better estimates of permeability for a particular rock unit and permeability range. Further work is required to improve methods for estimating permeability by PIA.

CONCLUSIONS

In summary, a medium-resolution petrographic image analysis system which can automatically measure grain and pore dimensions was developed. The system has the capability of measuring porosity and pore/grain dimensions from some thin sections. However, there are system limitations for measurements of small features less than 1 μm . Therefore, measurements of tight rocks or rocks with small pores are not candidates for PIA with the present optical microscope.

The following conditions must be adhered to if PIA measurements are to represent accurate pore properties.

1. The proper magnification must be used, and a sufficient number of images must be analyzed to obtain a statistically valid average of the rock features.

2. A high-contrast image must be obtained by appropriate sample preparation and microscopic image capture.

3. Proper selection of the image threshold by a trained operator must be made to create a binary image.

Considerable effort was made to improve the quality and contrast of fluorescent images from thin sections. However, some rocks containing significant quantities of silts and clays are not candidates for PIA using the fluorescent image process. A high-resolution color camera and further work are required to improve PIA data of porosity and specific surface area for

rocks containing significant quantities of silts and clays.

The application of image analysis for estimating permeabilities will require additional study. These studies would include obtaining an empirically derived Kozeny constant and using this constant for predicting permeabilities for a particular rock unit. It is also necessary to obtain accurate data by PIA for porosity, and specific surface area. This involves selecting the proper magnifications for porosity and surface area measurements. Also the permeability evaluations by PIA should be extended to both the few millidarcy and the few darcy ranges.

REFERENCES

1. Honarpour, Matt, Project Leader. Reservoir Assessment and Characterization, Final Report. Dept. of Energy Report No. NIPER-390, in press.
2. Davis, John C. Statistics and Data Analysis in Geology, 2nd ed., John Wiley and Sons, Inc., New York, 1986, p. 646.
3. Dullien, F. A. L. Porous Media, Fluid Transport and Pore Structure, Academic Press, New York, 1979, p. 396.
4. Carman, P. C. Trans., Inst. Chem. Eng., London, v. 15, 1937, p. 150.

TABLE 1. Measurements of microsphere diameters by image analysis

Manufacturer specifications		Image analysis	
Mean diameter, μm	Std deviation, %	Mean diameter, μm	Std deviation, %
32.2	10.0	32.3	0.3
9.8	11.2	10.2	4.4
6.8	13.0	6.9	10.3
3.8	21.0	3.3	18.3

TABLE 2. - Porosity measured by volumetric analysis of core plugs and porosity from thin section PIA (10X objective)

<u>Formation</u> Sample number	Volumetric porosity, %	Mean PIA porosity, %	Standard deviation of 40 images by PIA, %
<u>Muddy Outcrop</u>			
23 125 62	28.9	29.6	7.4
386 0 1	20.7	20.8	6.6
23 155 10	33.3	33.5	6.5
386 0 10.5	33.5	33.6	4.3
22 625 2	21.7	20.3	8.2
23 183 15	9.3	11.5	5.3
386 55 16.5	25.8	27.6	6.2
23 155 4	30.6	26.3	6.3
23 155 1	21.4	22.0	6.7
386 0 5	35.7	33.2	5.7
23 625 16.5	28.4	30.3	5.5
<u>Hartzog Draw Field</u>			
5308 9382	15.6	8.4	4.4
5308 9394	13.6	12.8	7.5
5308 9368	15.9	17.9	9.5
5308 9370	16.1	8.4	4.4
5308 9414	6.3	12.4	3.5
5308 9404	12.1	10.4	4.0
<u>Shannon Outcrop</u>			
135 30	35.8	24.7	5.7
151 13	23.3	15.7	6.7
157 9	29.6	24.7	4.5
125 32	31.2	23.0	5.7
172 -1	25.1	21.3	7.6
<u>Naval Reserve Field B-3</u>			
(A)-8	29.5	27.8	6.8
(B)-1	22.3	22.6	13.1
(B)-4	26.5	25.2	10.9
(B)-9	28.2	25.9	6.5
(B)-6	28.6	26.9	5.7
(A)-6	25.9	27.8	8.9
(A)-7	29.5	28.2	6.3
(B)-12	24.9	21.6	7.4

TABLE 3. - Measurements of rock grains for maximum and minimum mean diameters and mean grain area

Thin section identification	Mean area, μm^2	Mean diameter, μm		Mean perimeter, μm
		maximum	minimum	
22-100-6.5	6,259	108.2	61.3	369.9
22-100-8	8,390	121.9	72.7	431.9
22-100-8.5	6,588	107.7	63.1	370.0
22-100-12.5	9,489	123.1	74.1	424.3
C4-4361.5	8,691	124.8	71.1	437.3
W7-4428.5	6,909	108.2	62.0	371.0
W11-4366.9	7,141	108.6	60.4	357.4
W11-4378.7	9,553	129.8	74.0	450.4

TABLE 4. - Comparison of grain area with elliptical area based on maximum and minimum grain diameters

Thin section identification	Actual area		Ellipse area		Regression analysis		
	Average	Standard deviation	Average	Standard deviation	Intercept	Slope	R-squared
	μm^2	μm^2	μm^2	μm^2			
22-100-6.5	6259	4144	5813	4015	-101.3	0.9449	0.9511
22-100-8	8390	6019	7906	5867	-108.7	0.9553	0.9605
22-100-8.5	6588	4774	6179	4663	-113.3	0.9551	0.9563
22-100-12.5	9489	11773	9061	12068	-572.9	1.0153	0.9809
C4-4361.5	8691	7238	8244	7230	-249.2	0.9774	0.9574
W7-4428.5	6909	7153	6435	6950	-181.5	0.9578	0.9715
W11-4366.9	7141	5886	6665	5628	-107.1	0.9484	0.9709
W11-4378.7	9553	10212	9022	10384	-554.8	1.0025	0.9721

TABLE 5. - Comparison of porosity and permeability obtained by PIA with those obtained by core plug analysis using the Kozeny constant of 5

Thin section	Plug		5X Objective			10X Objective		
	porosity, %	permeability, md	PIA porosity, %	PIA permeability, md	Specific surface, m^{-1}	PIA porosity, %	PIA permeability, md	Specific surface, m^{-1}
B1	22.3	289	25.0	304	0.1349	22.6	132	0.1714
A6	25.9	522	25.0	415	0.1162	27.8	648	0.1130
B12	24.9	950	28.8	915	0.1017	21.6	146	0.1502
B4	26.5	462	26.3	449	0.1225	25.2	424	0.1163
B9	28.2	852	26.5	505	0.1170	25.9	277	0.1510
A7	29.5	647	27.1	567	0.1151	28.2	583	0.1226
B2	28.6	1051	27.1	524	0.1192	25.9	270	0.1526
A8	29.5	2077	26.5	726	0.0976	27.8	706	0.1083

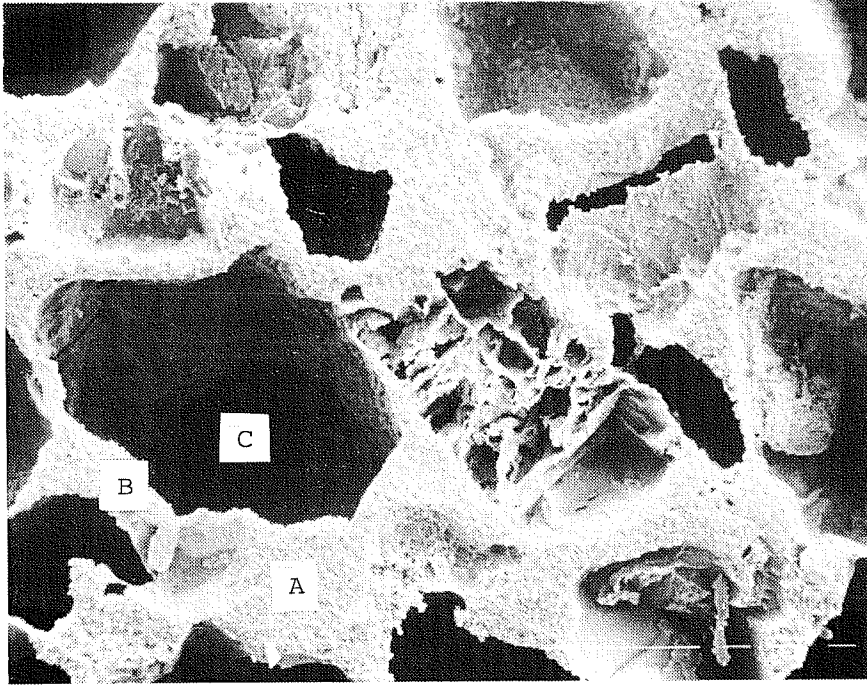


FIGURE 1. - SEM backscattered electron image of epoxy pore cast of a sample from Bell Creek field, Powder River County, Montana. Width of image is 160 μm . The image shows the shape and size of the pore structure (lighter gray) and rock matrix (darker gray).

(A) shows the larger pores, (B) shows pore connectivity, and (C) smaller secondary porosity resulting from silt and clay inclusions.

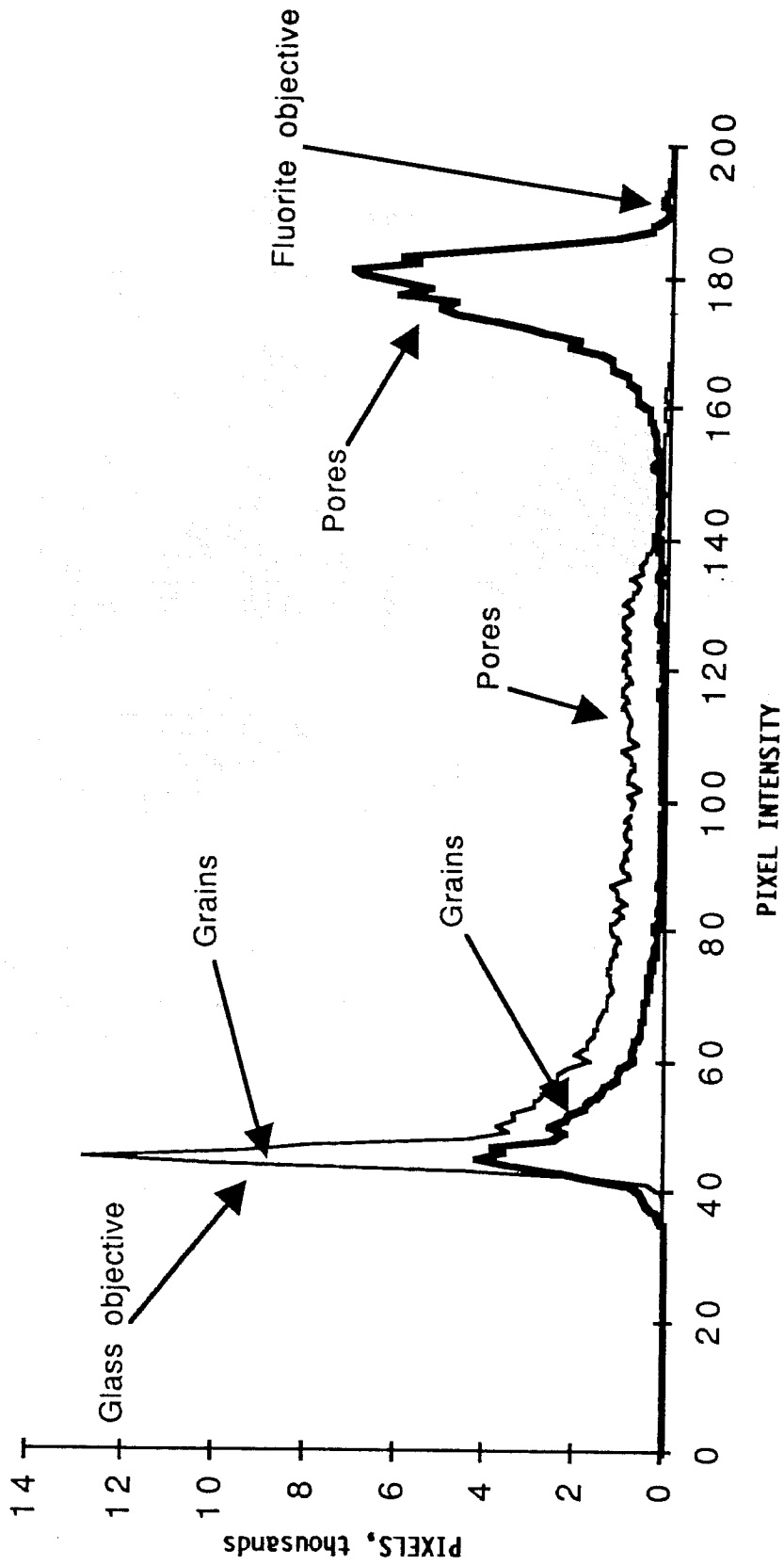


FIGURE 2. - Pixel intensity histogram showing contrast of images captured using glass and fluorite objectives. Black is represented by zero pixel intensity value while full white by 255 pixel intensity values. The fluorite objective has higher fluorescent intensity and better pore/grain contrast.

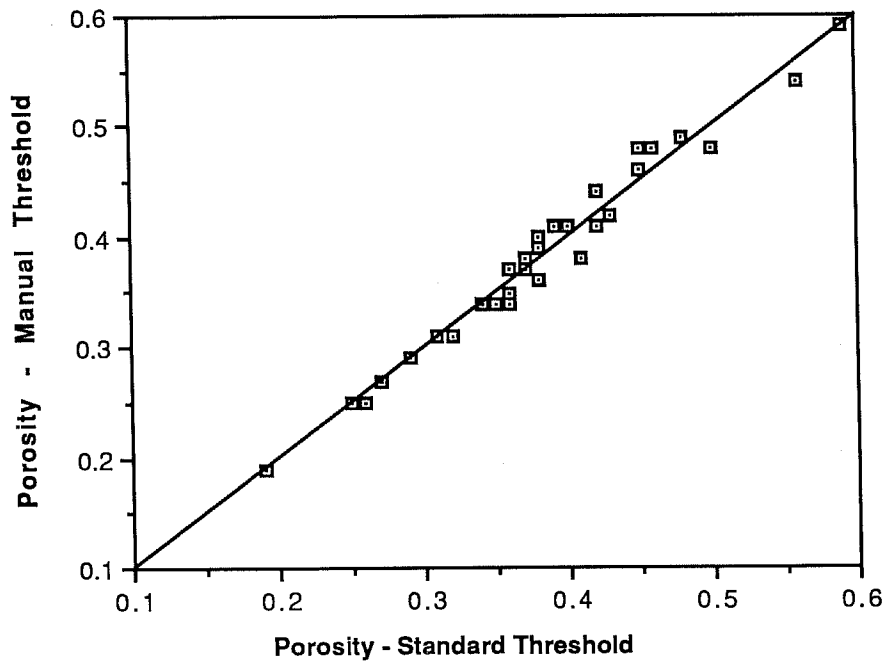


FIGURE 3. - An example of porosity area variation due to thin section heterogeneities (thin section W14 4297.7). The figure also shows the difference in porosity area measurements obtained by using a single, standard threshold for all porosity measurements versus threshold adjustment for each captured image.

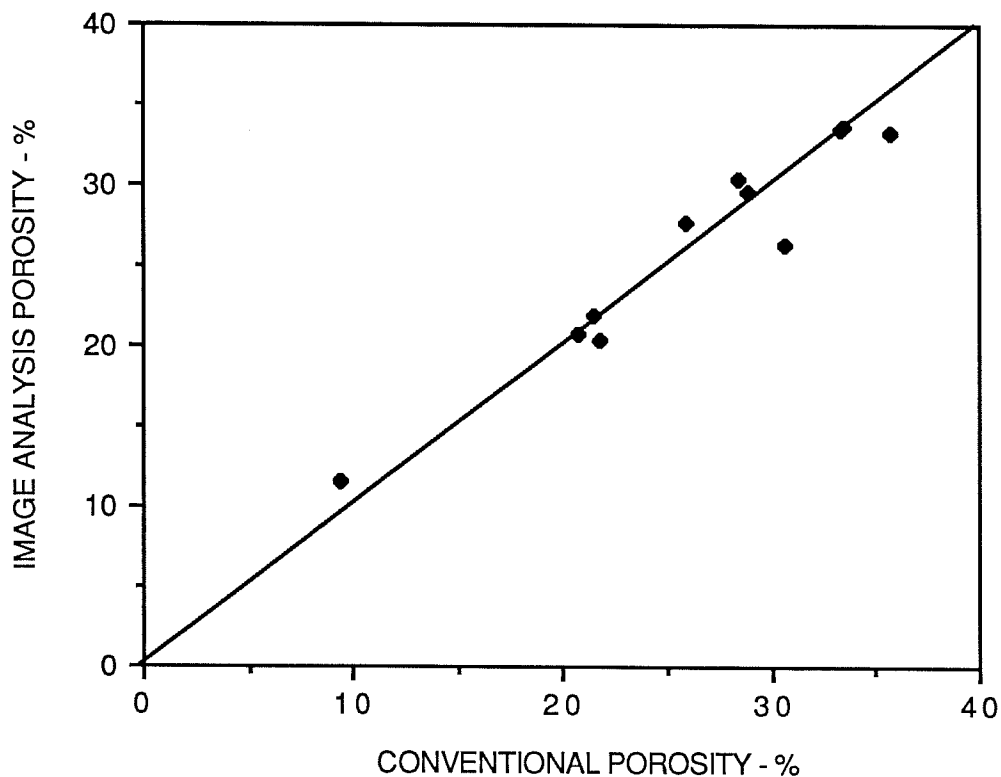


FIGURE 4a. - Correlation of image analysis porosity versus volumetric core-plug analysis for Muddy formation.

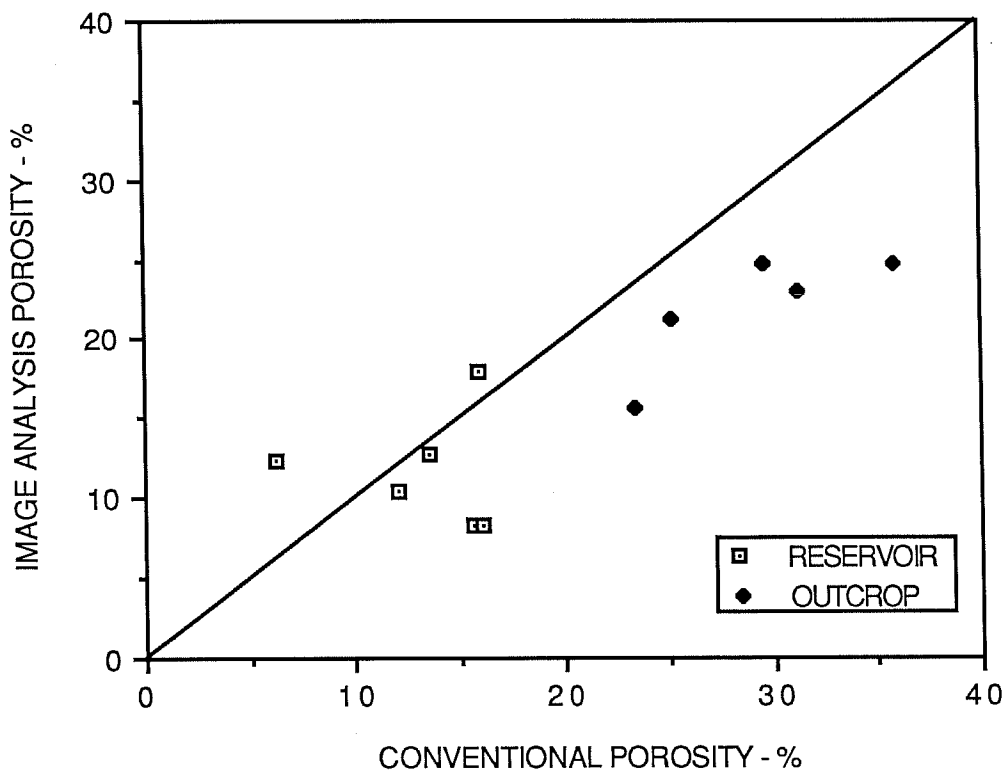


FIGURE 4b. - Correlation of image analysis porosity versus volumetric core-plug analysis for Shannon formation.

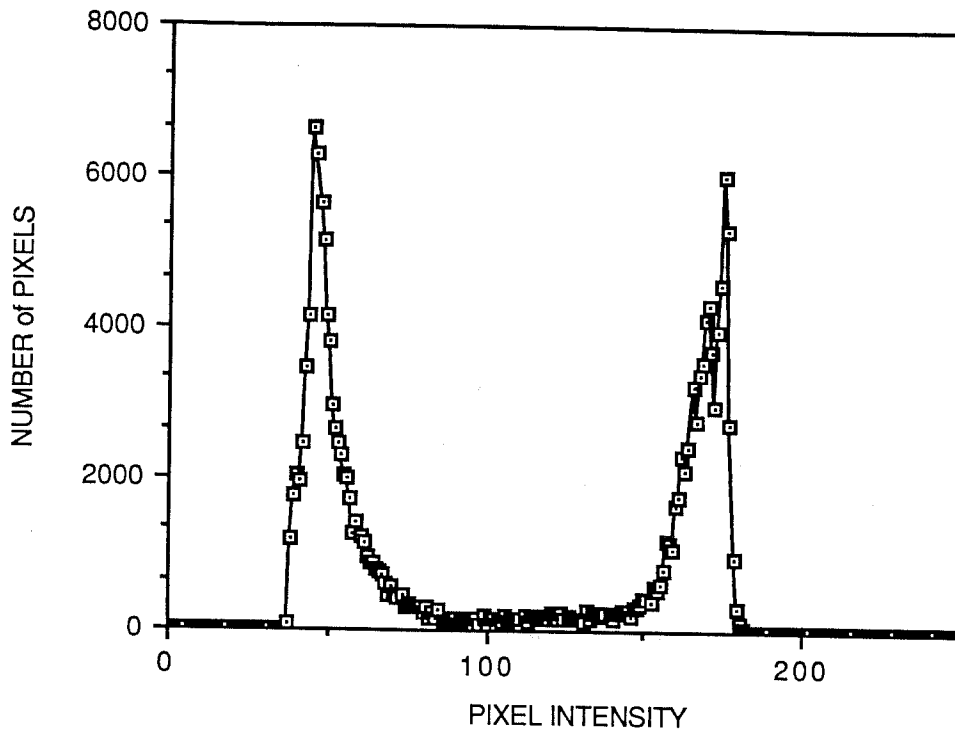


FIGURE 5a. - Histogram of pixel gray-level for fluorescent image of a "clean" sandstone.

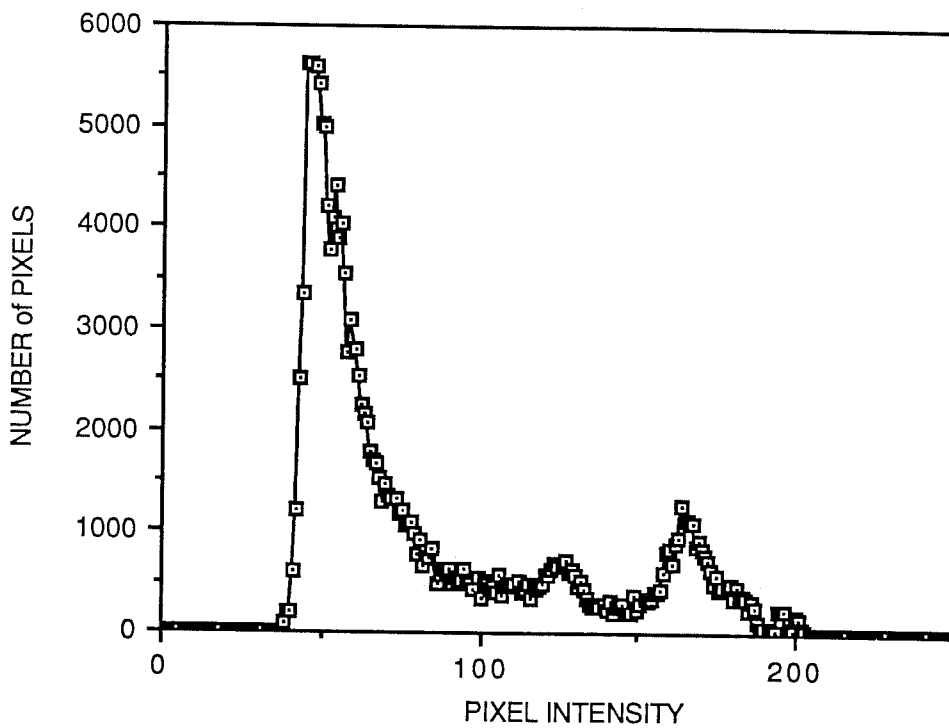


FIGURE 5b. - Histogram of pixel gray-level for a fluorescent image of a low-porosity sandstone containing large quantities of clays and silty materials.

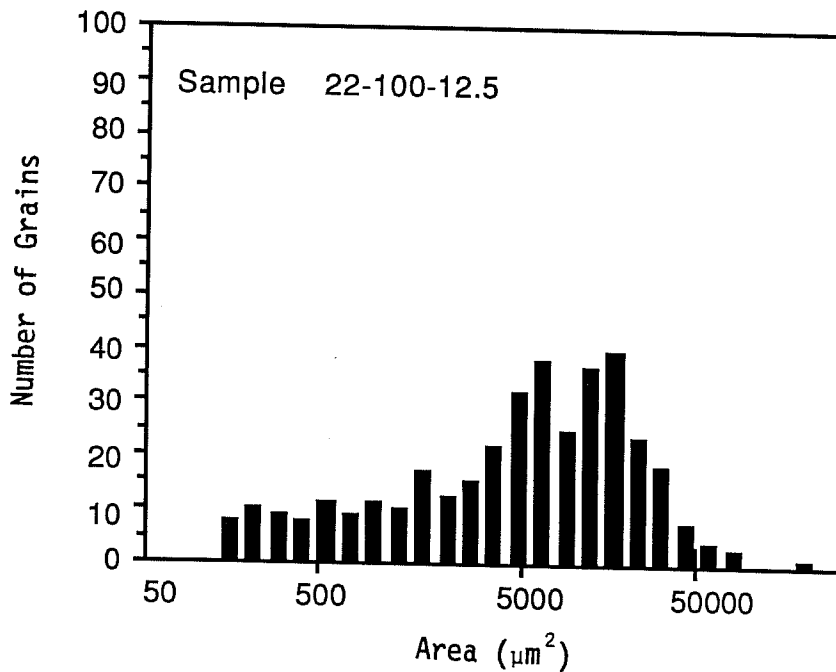
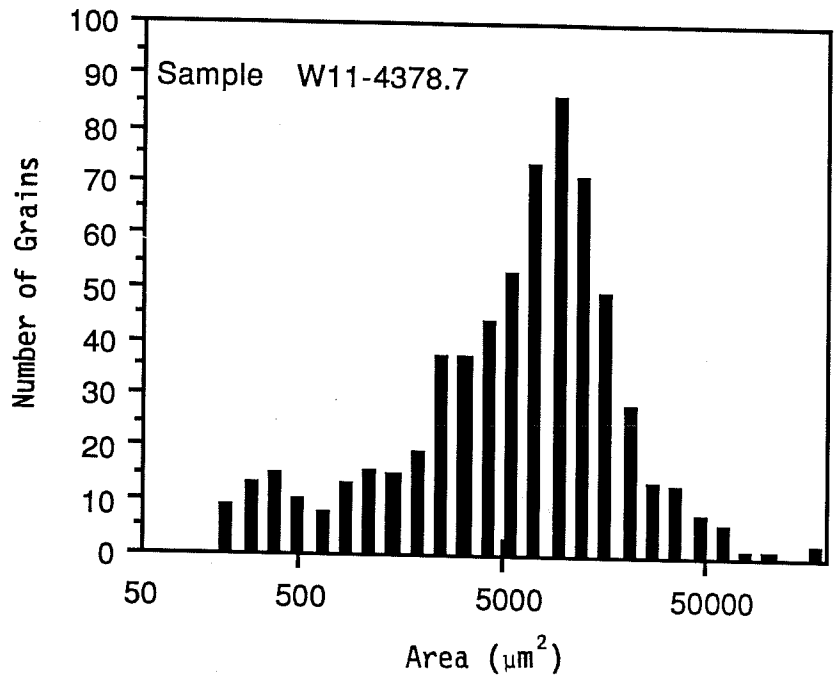


FIGURE 6. - Comparison of grain areas for two thin sections from subsurface (W11-4378.7) and outcrop (22-100-12.5)

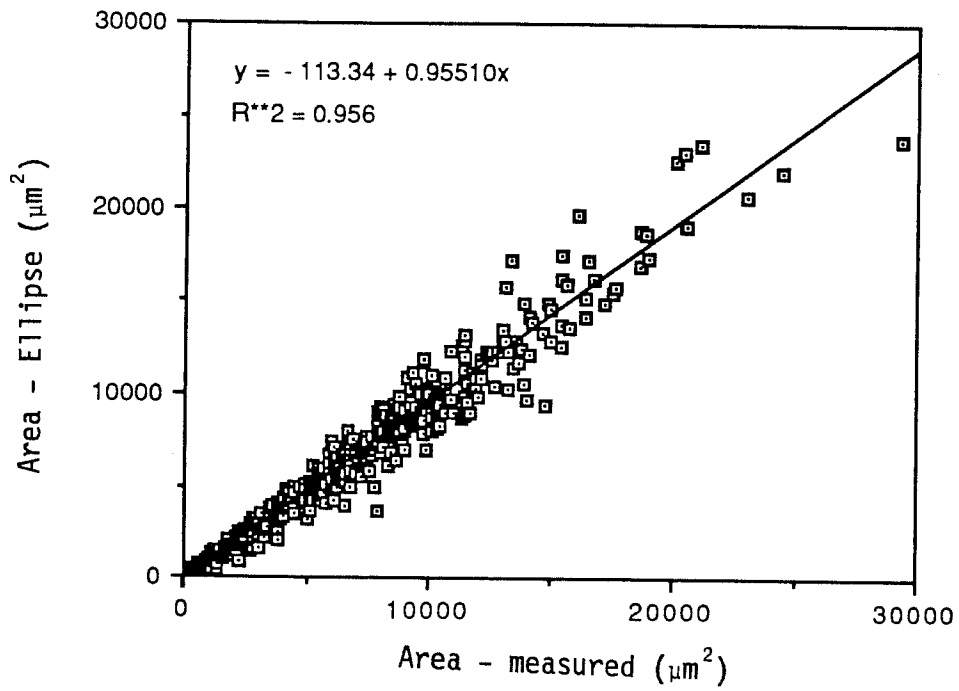


FIGURE 7. - Comparison of elliptical area based on maximum and minimum grain diameters with measured grain areas.

